

“Frontier of EQ prediction studies” (tentative title) M. Hayakawa, editor

Electric Currents in the Earth Crust and the Generation of Pre-Earthquake ULF Signals

Friedemann Freund^{1,2,3} and Stuart Pilorz²

¹ NASA Ames Research Center, Earth Science Division, MS 232-4
Moffett Field, CA 94035, USA
friedemann.t.freund@nasa.gov

² SETI Institute, Carl Sagan Center, 189 Bernardo Ave.
Mountain View, CA 94043, USA

³ San Jose State University, Department of Physics
San Jose, CA 95192-0106

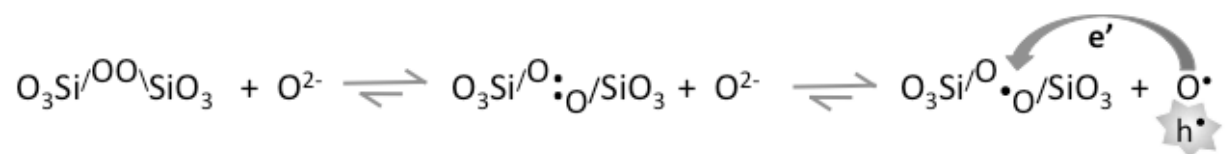


Figure 1: Peroxy bond breakage and generation of a positive hole, h^\bullet , which becomes a mobile electronic charge carrier.

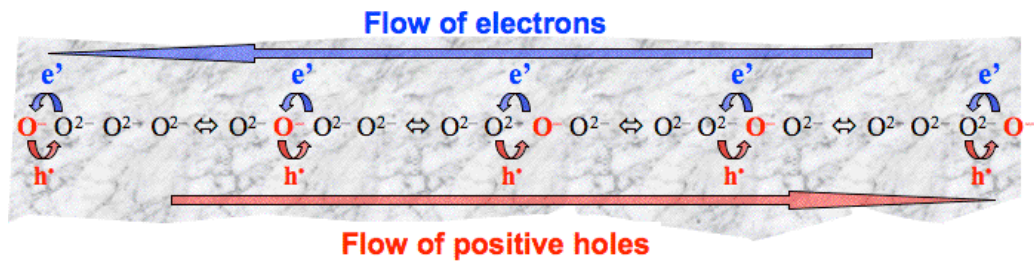


Figure 2: Principle of phonon-mediated electron transfer as the basic mechanism by which positive holes can propagate through the matrix of a mineral grain.

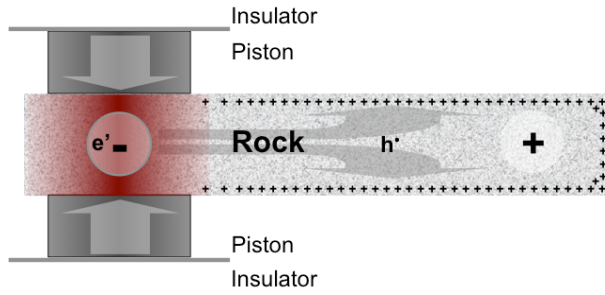


Figure 3a: The stressed rock volume turns into a source of charge carriers. Mechanical work is done to activate the charge carriers. The positive holes h flow into the unstressed rock, creating an electrical potential.

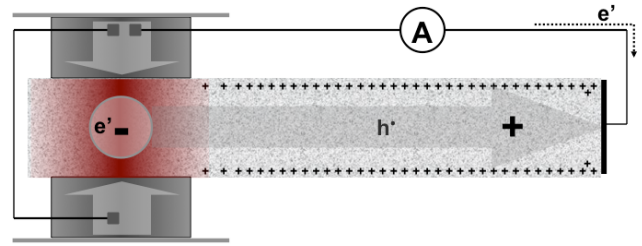


Figure 3b: The battery circuit can be closed by running a wire from the pistons (which are in electrical contact with the stressed rock) to the unstressed end of the rock. This wire allows electrons to flow out of the stressed subvolume.

Figure 3c: *Analog to an electrochemical battery where the positive current leg is carried by cations flowing through an electrolyte. The anode and the electrolyte are chemically different. Energy is stored in the form of chemical energy and is released through chemical reactions at the anode-electrolyte and cathode-electrolyte interfaces.*

Figure 4: *Schematic cross section through the Earth crust with a general description of the mechanical and electrical properties as a function of temperature with increasing depth, e.g. along the geotherm. The most important aspect is the postulated p-n transition at a depth corresponding to a temperature of 500-550°C.*



Figure 5a: *Depiction of a tectonic stress field building up across the entire Earth crust, marked by isobars (red curves) and by the outflow of positive hole charge carriers, h^+ , ahead of the stress front (white arrows). The h^+ outflow also leads to a positive surface/subsurface charge.*

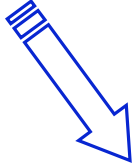


Figure 5b: *Depiction of a more advanced stage of the stress build-up across the Earth crust with the dynamically evolving isobars extending downward and crossing the postulated p-n boundary. Electrons flowing out of the stressed volume into the n-type lower crust and closing the battery circuit (not to scale).*

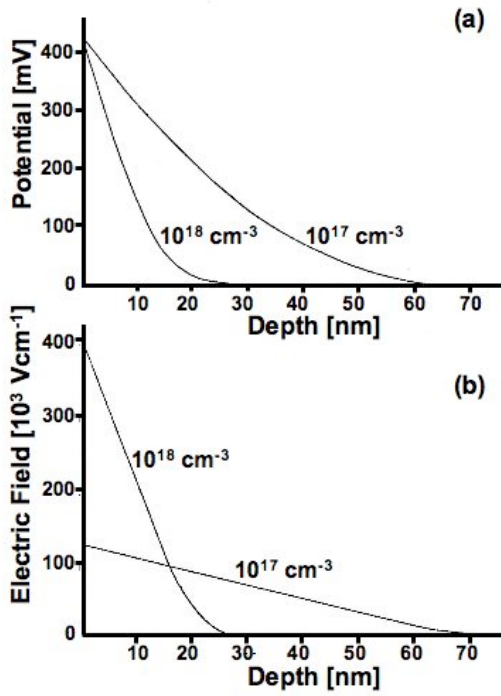


Figure 6a/b:

Calculated surface/subsurface potential and electric field for a semi-infinite dielectric with $\epsilon=10$ with mobile positive hole charge carriers at two concentration levels, 10^{17} and 10^{18} cm^{-3} , equivalent to 10 and 100 ppm relative to the number of oxygen anions per unit volume [King and Freund, 1984].

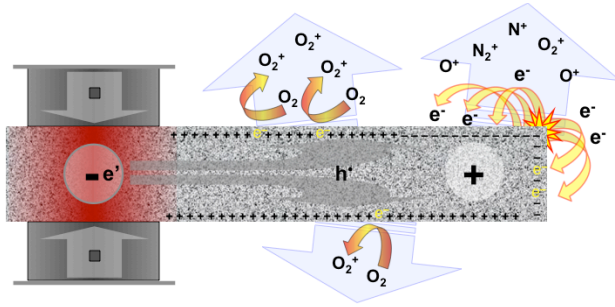


Figure 7a: Depiction of (i) field-ionization of air molecules, probably O_2 , and (ii) corona discharges at the surface of a rock stressed at one end [Freund et al., 2009].

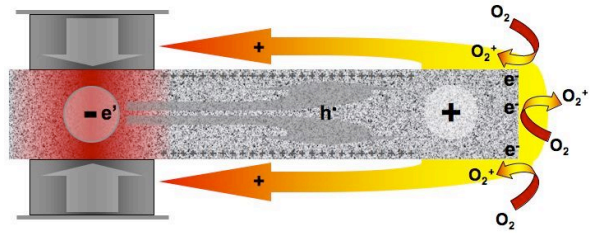


Figure 7b: Depiction of the postulated ion current flowing through the air as a possible pathway to close the battery circuit

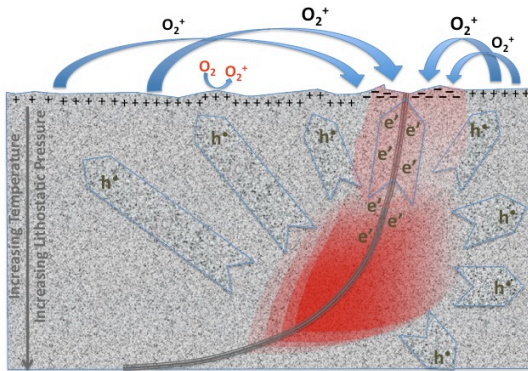


Figure 8: Concept drawing of a situation where a epicenter of an impending earthquake that develops in a shallow portion of the crust creates an area of a negative surface charge (due to corona discharges) surrounded by a halo of positive surface charge. Positive airborne ions generated by field-ionization at the outer halo are shown to form a ion current through the air, which closes the battery circuit.

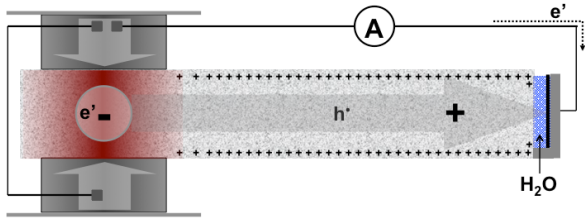


Figure 9a: Basic set-up to demonstrate that stress-activated h^+ currents can flow into water and close the battery circuit.

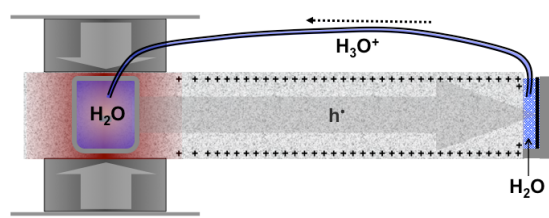


Figure 9b: Demonstration of a rock battery where the circuit closure is achieved through the electrolytical conductivity of water.

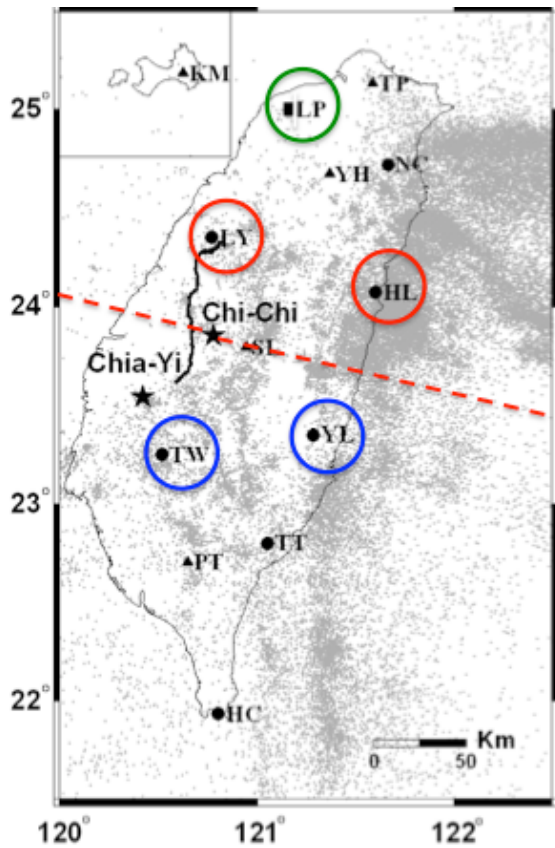


Figure 10a: Map of Taiwan [Yen et al., 2004]. The black solid line marks the surface rupture. The gray dots mark earthquake epicenters for seismic events with $M \geq 3$. The two black stars indicate the locations of the Chi-Chi main shock and of Chia-Yi aftershock, with which the aftershock series ended. The locations of the magnetometer stations of the island-wide geomagnetic network are denoted by solid circles (stations at the time of the Chi-Chi earthquake), and solid triangles (newer stations). Data from the two pairs of stations circled in red and blue, LY-HL and TW-YL respectively, will be discussed here in greater detail. The black rectangle in the North, circled in green, indicates the location of the reference station LP. The dashed red line marks the approximate location of the cross section in **Figure 10b** (modified after [Yen et al., 2004]).

Tectonic Setting Chi-Chi Earthquake Taiwan (schematic)

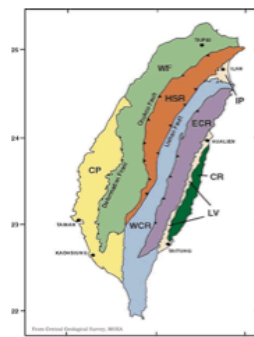
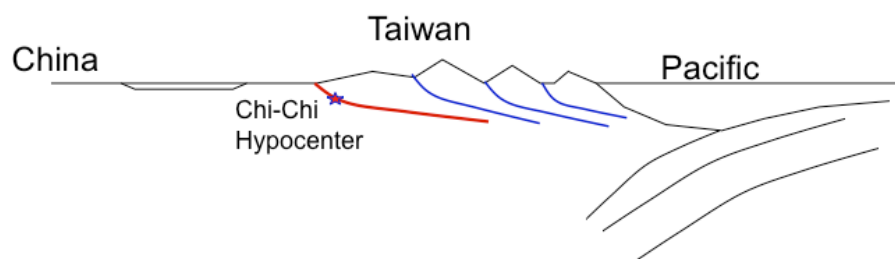


Figure 10b: Tectonic map of Taiwan and E-W cross section at the approximate location of the Chi-Chi hypocenter on the Chelungpo Fault (red).



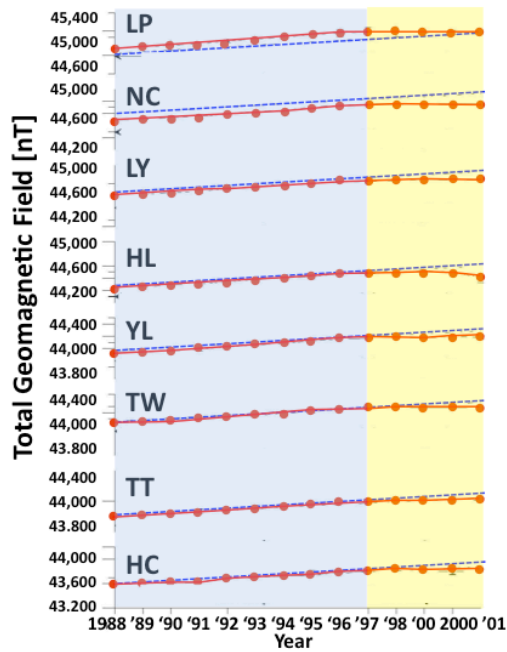


Figure 11a: Longterm trend of the regional magnetic field recorded at the Taiwan magnetometer station network (yearly averages: red line and red circles) compared to the IGRF model prediction (modified after [Chen et al., 2004b; Yen, 2004]).

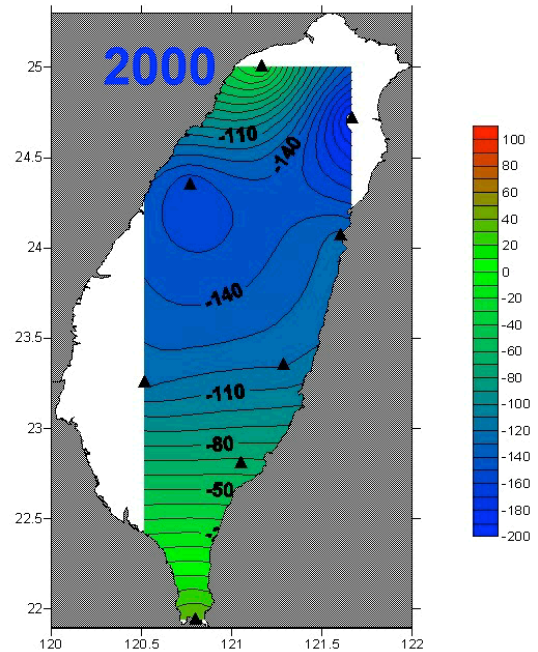


Figure 11b: Total magnetic field anomaly across Taiwan for 2000 relative to the linear extrapolation of the long-term trend predicted by the IGRF model (after [Chen et al., 2004b; Yen, 2004]).

Electrolytical Circuit Closure

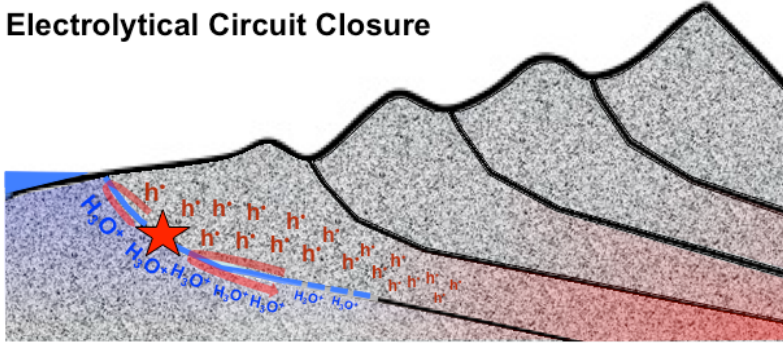


Figure 12: Schematic E-W cross section of Taiwan to illustrate the concept of the electro-lytical conductivity of a water/brine-saturated fault capable of closing the battery circuit (red hues: dynamic stress build-up due to thrust from the right).

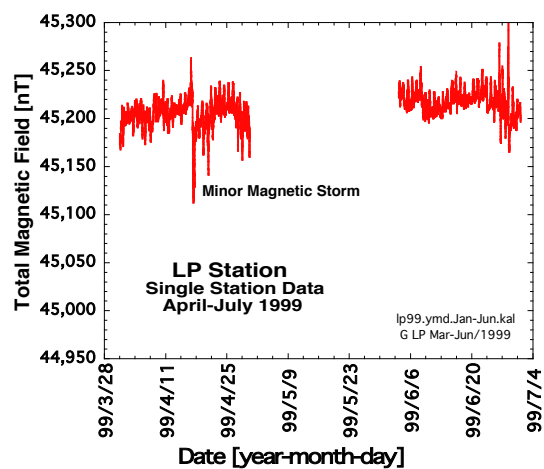


Figure 13a: Total magnetic field recorded at the LP station over parts of a 96-day period in early 1999.

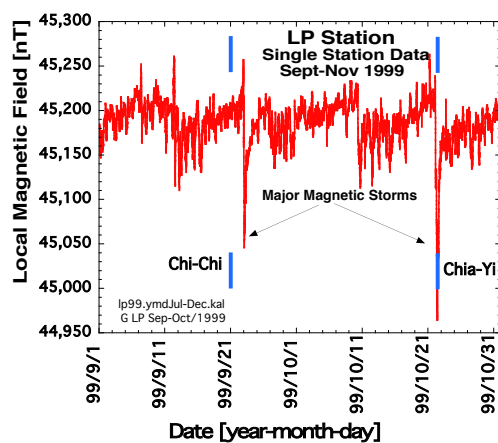


Figure 13b: Total magnetic field recorded at the LP station over 2 months in late 1999. Blue lines: Chi-Chi and Chai-Yi events.

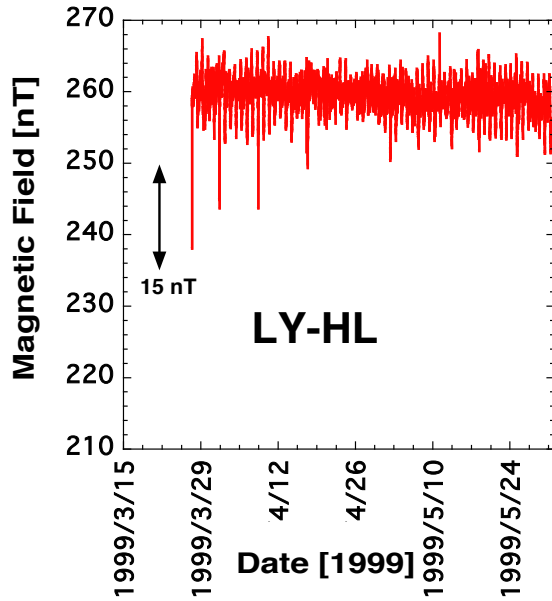


Figure 14a: Small magnetic field residuals obtained from the difference of magnetic data recorded at the LY station minus those of the HL station over 2 months in early 1999.

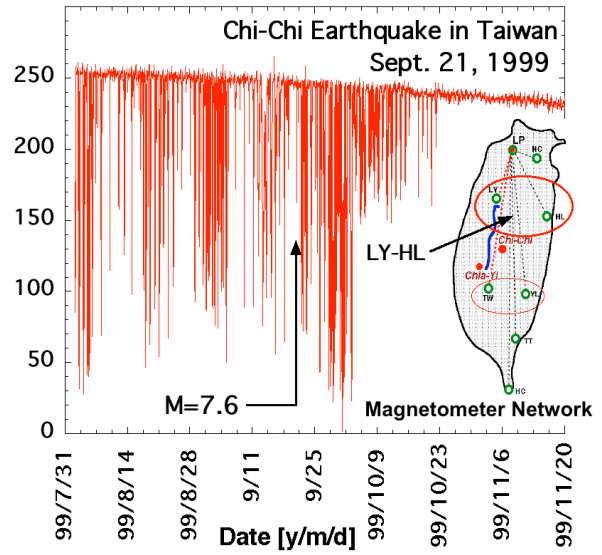


Figure 14b: Large magnetic field residuals seen in the data from the LY minus HL station data for the period from Aug. 01, 1999 to Nov. 20, 1999.

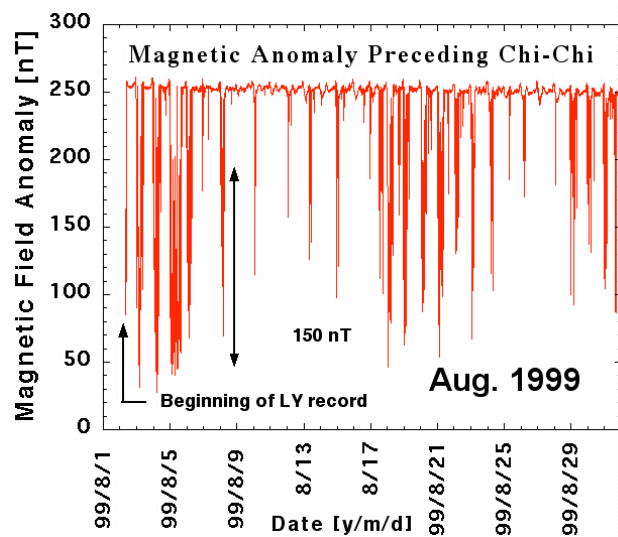


Figure 15a: LY-HL record for Aug. 1999.

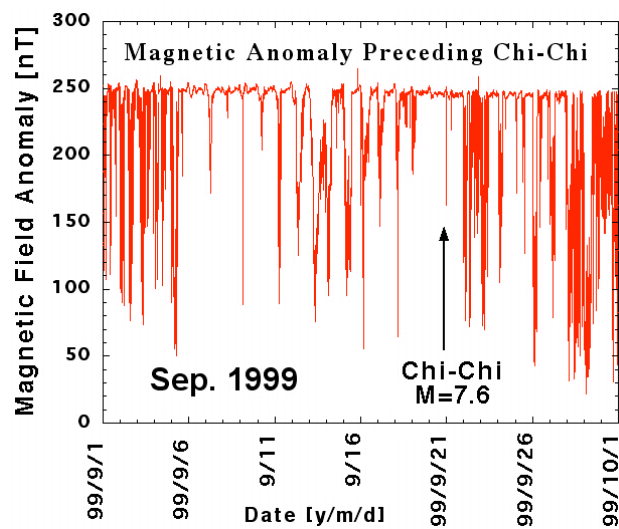


Figure 15b: LY-HL record for Sep. 1999.

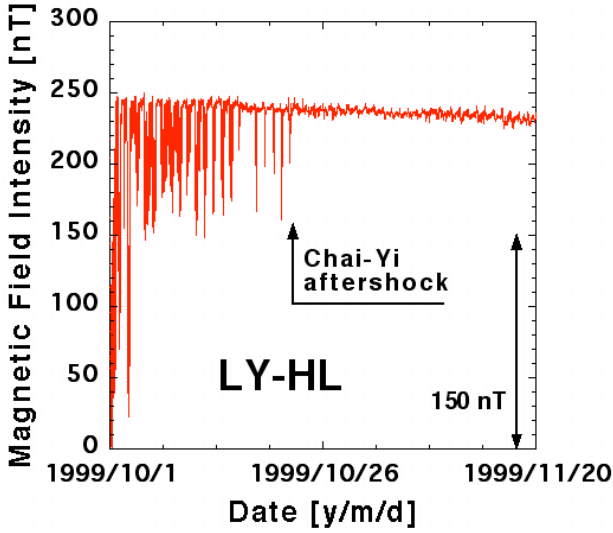


Figure 16a: LY-HL data for the period after the Chi-Chi main shock, including the major aftershock at Chai-Yi on Oct. 22, 1999, when the ULF activity recorded at the LY station faded away.

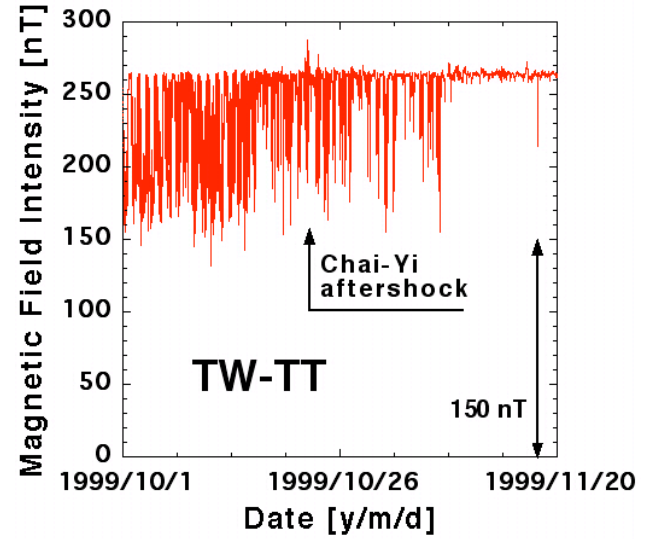


Figure 16b: TW-TT data for the period beginning 4 days after the Chi-Chi main shock and extending beyond the Chai-Yi aftershock, showing continuing ULF activity at TW station.

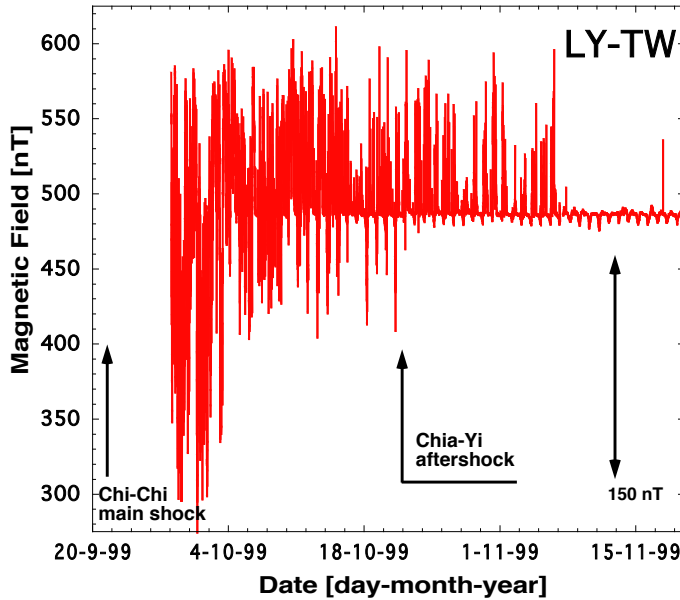


Figure 16c:

LY-TW data to illustrate the shift of the ULF activity from the northern LY station toward the TW station south of the Chelongpu fault rupture.

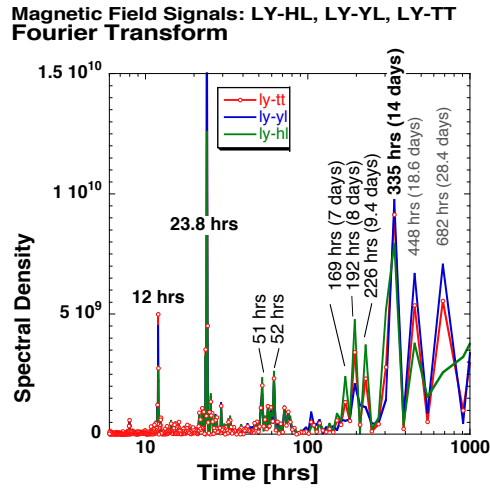


Figure 17: Spectral density of the ULF signals before the Chi-Chi main shock from a Fourier Transform as derived from the LY-HL, LY-YL, and LY-TT station data. The 7-week record is not long enough to provide accurate positions for the FT maxima, but the general pattern observed indicates strong control by the Earth tides.

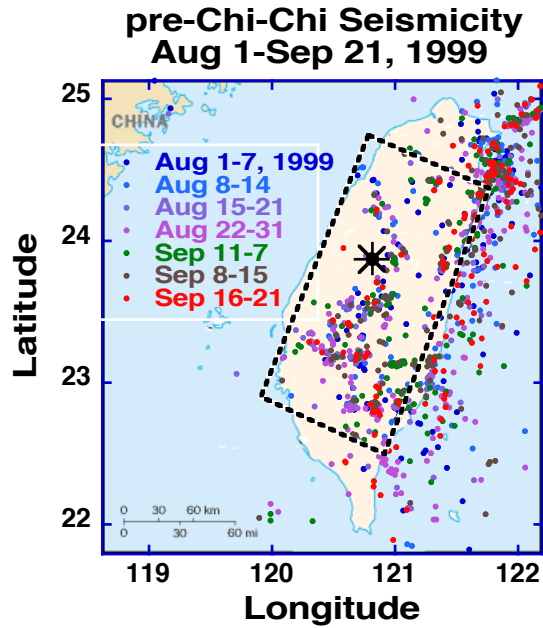


Figure 18a: Low-magnitude seismic activity during the 7 weeks before the Chi-Chi main shock, color-coded by week. Rectangular box selected arbitrarily most of Taiwan.

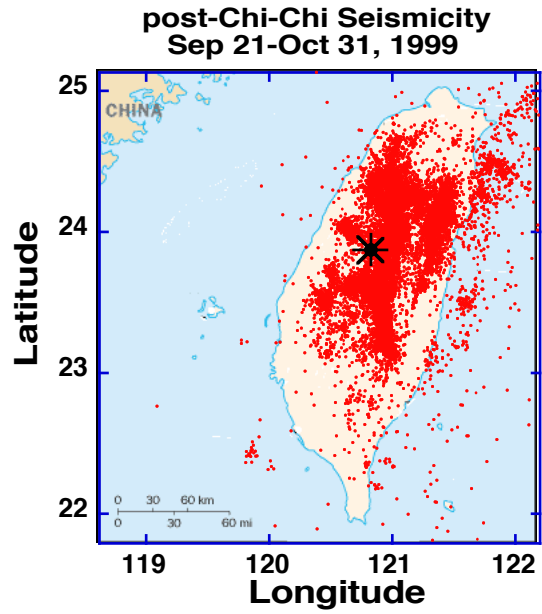


Figure 18b: Total Chi-Chi seismic activity during the period between the Chi-Chi main shock and the Chai-Yi aftershock.

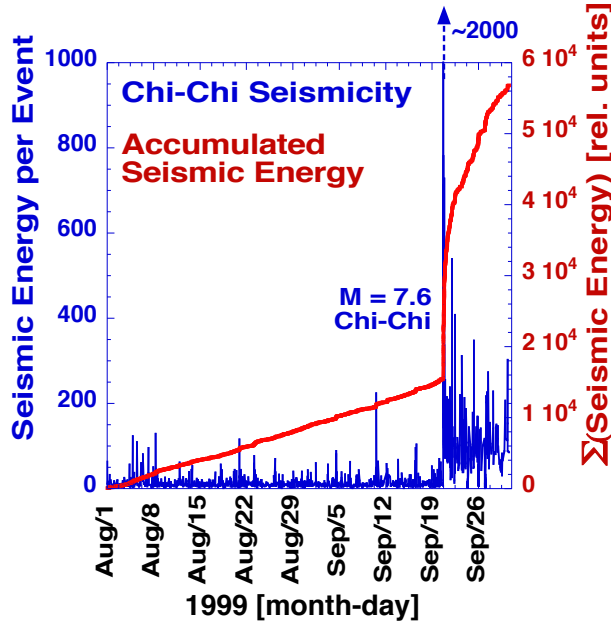


Figure 19a: Seismic energy, defined as 10^M with M = magnitude, released before, during and immediately after the Chi-Chi mainshock (blue). Summation of seismic energy (red).
Data: Taiwan earthquake catalog

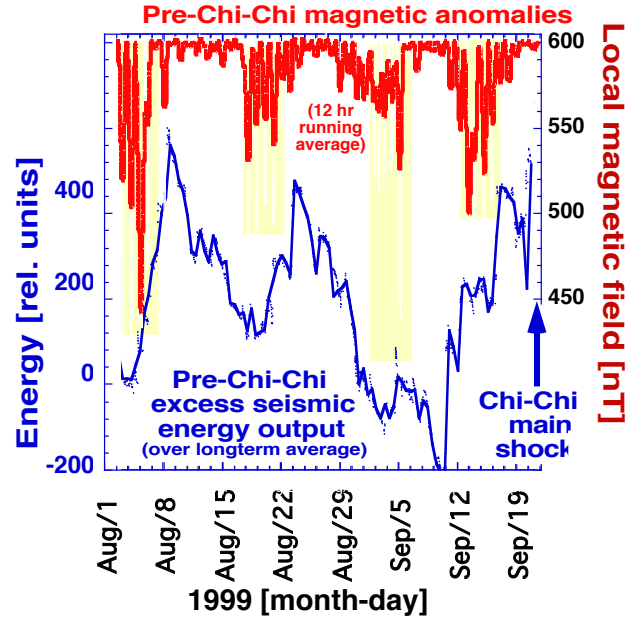


Figure 19b: Excess seismic energy release over the long-term average (blue) and ULF signals recorded at the LY station (red) showing a correlation with the Earth tides. Yellow bands highlight the ULF maxima.

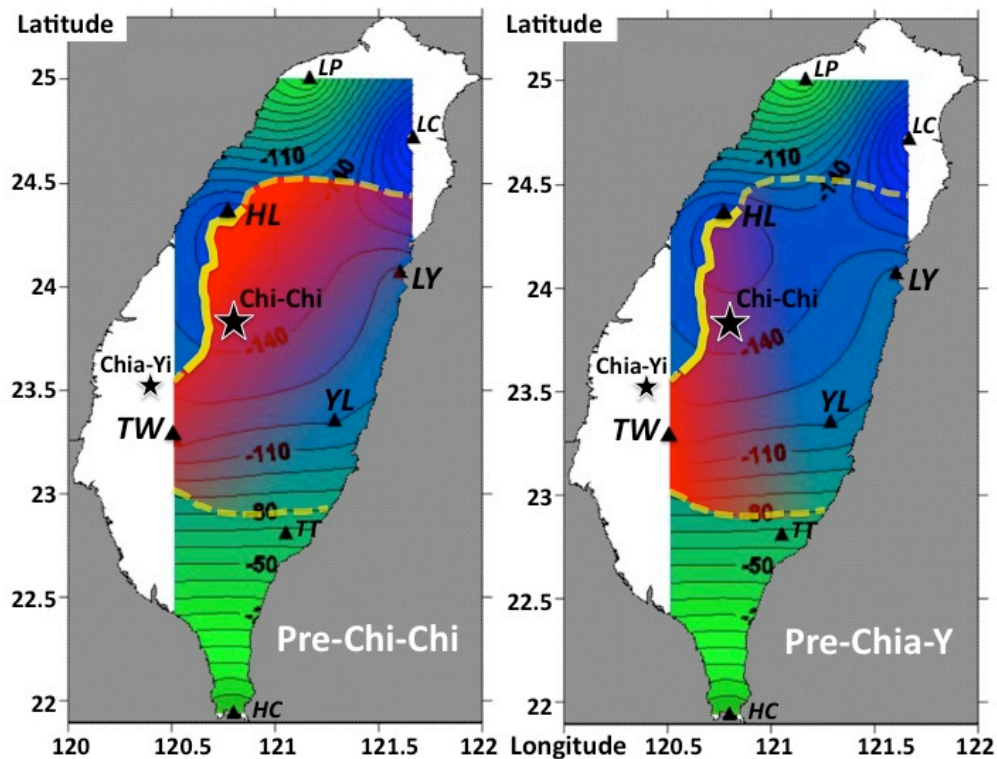


Figure 20a: Superposition of a postulated electric current field over the magnetic field anomaly across Taiwan for the pre-Chi-Chi period. Red hues: electric current intensity.

Figure 20b: Superposition of a postulated electric current field over the magnetic field anomaly across Taiwan for the pre-Chia-Yi period. Red hues: electric current intensity.

